

2

cERL

2-1 cERL Overview

To demonstrate the generation and recirculation of low-emittance and high-current beams that are required for the 3-GeV ERL project (PEARL) [1], the Compact ERL (cERL) [2] has been constructed at KEK. The cERL consists of a 5-MeV injector, a 30-MeV main linac, and a recirculation loop. The principal parameters of the cERL are given in Table 1.

High-brightness electron beams are produced in the photocathode DC electron gun of the injector. The beams are accelerated up to a nominal energy of 5 MeV using a superconducting (SC) injector cryomodule. The beams are merged with the SC main linac where they are accelerated to a nominal energy of 35 MeV, and then are transported through the recirculation loop. The beams are then decelerated in the main linac, and are dumped. The beams from the injector can also be transported through the injector-diagnostic beamline where various beam properties can be measured.

The injector was constructed in FY2012, and was completed in April, 2013. Commissioning of the injector was carried out from April to June, 2013 [3]. During this period, we demonstrated the production and acceleration of low-emittance beams, which is described in the next section. We also demonstrated stable operation of the injector including the photocathode DC gun under a cathode voltage of 390 kV as well as the SC cavities of the injector with a typical accelerating gradient of 7 MV/m. The total beam-operation time during the injector commissioning was approximately 202 hours.

From July to November, 2013, we constructed the recirculation loop of the cERL [4]. First, base plates for the magnets were installed in the cERL accelerator room (radiation shielding). Next, the magnets including eight bending magnets and 60 quadrupole magnets with their girders were installed. The magnets were then precisely aligned using both a laser tracker and a tilting level; 40 surveying references, which were located at the inner walls of the accelerator room, were used as references. In this installation process, the magnets were aligned within ± 0.1 mm in position and within ± 0.1 mrad in angle. The upper parts of the magnets were then removed, and all vacuum chambers were

installed. Thirty screen monitors and 45 stripline beam-position monitors (BPMs) were also installed. After the magnets were reassembled, it was found that the magnets were aligned less accurately (mostly, ± 0.5 mm in position and ± 0.5 mrad in angle), however, we did not realign the magnets due to limited time.

The main-linac cryomodule having two nine-cell SC cavities was installed in FY2012. During the high-power test, the two cavities achieved accelerating voltages of 14.2 MV and 13.5 MV, respectively, for more than 1 hour. However, field emissions emerged at an accelerating voltage of about 8 MV. Then, we decided to start commissioning of the entire cERL with an accelerating voltage of 8.5 MV/cavity, by which the beam energy in the recirculation loop was determined to be 20 MeV.

We also installed power supplies for the magnets, as well as the electronics for the beam diagnostic system, vacuum system, and so on, outside the accelerator room. The construction of the cERL was completed in November 2013. The present (at the end of FY2013) layout of the cERL is shown in Fig. 1. Figures 2 and 3 show photographs of the cERL.

From December 2013 to March 2014, we commissioned the entire cERL. During this period, electron beams were successfully recirculated through the recirculation loop, and were decelerated and transported to the beam dump with small beam losses. The maximum beam current of about $6.5 \mu\text{A}$ was achieved under continuous-wave (CW) operation. The principal parameters achieved during this period are given in Table 2. In the next section, the commissioning of the cERL is reported in detail. With these achievements, we are going to the next stage with high-bunch-charge or high-current operations which are needed to construct the 3-GeV ERL.

REFERENCES

- [1] "Energy Recovery Linac Conceptual Design Report", *KEK Report 2012-4* (2012)
<http://ccdb5fs.kek.jp/tiff/2012/1224/1224004.pdf>
- [2] S. Sakanaka *et al.*, *Proc. of IPAC13*, 2159 (2013).
<http://accelconf.web.cern.ch/AccelConf/IPAC2013/index.htm>
- [3] S. Sakanaka *et al.*, *Proc. of ERL2013*, 16 (2013).
<http://accelconf.web.cern.ch/AccelConf/ERL2013/index.htm>
- [4] N. Nakamura *et al.*, *Proc. of IPAC14*, 353 (2014).
<http://inspirehep.net/record/1314288?ln=ja>

2-2 Commissioning of cERL

2-2-1. Commissioning of Injector beam line

The beam commissioning of the cERL was carried out in two steps. First, the injector beamline, which consists of a photocathode DC gun, two solenoid magnets, a bunching cavity, superconducting injector cavities, five quadrupole magnets, and a beam diagnostic line to measure the injector beam performance, was placed into operation. The maximum beam energy and current were limited to 6 MeV and 1 μA , respectively. In the second step, we constructed a merger section and a recirculation loop with main superconducting cavities, and operated the whole ERL to demonstrate energy recovery without beam loss. In the second step, the maximum beam energy and current were increased to 35 MeV and 10 μA , respectively.

From 22 April 2013 to 28 June 2013, we carried out the beam commissioning of the cERL injector beamline to demonstrate high-quality beam generation from the photocathode gun, beam acceleration by the injector superconducting cavities, and beam transportation without degradation of beam quality. The photocathode gun, which was developed by JAEA, was operated at 390 kV. Although the maximum gun voltage was 500 kV, which was demonstrated at JAEA, it was reduced to 390 kV to avoid the discharge around the ceramic insulator. As a photocathode material, we employed a GaAs photocathode with NEA surface to generate a low-emittance beam. In order to confirm the low-emittance beam generation from the photocathode gun, we measured the transverse emittance using the solenoid scan method for very low bunch charge operation with 10 fC. The measured normalized emittance was 0.07 mm mrad, which was almost the same as the expected value from the GaAs photocathode.

The 390-keV electron beam was accelerated by the

injector superconducting cavities. After phase tuning of the cavities, we succeeded in accelerating the beam to 5.6 MeV with the acceleration field gradient of 7 MV/m. It only took 5 days to generate, accelerate and transport the electron beam to the beam dump without beam loss. On 23 May 2013, a radiation safety inspection of the injector beamline was performed with the average current of 200 nA, and we received a certificate of passing the inspection on 27 May 2013.

After the radiation safety inspection, we continued the beam operation for hardware performance tests, beam quality measurements, and fine beam tuning. The summaries of these are as follows. The photocathode gun operation was very stable, and there was no discharge during the injector commissioning. The injector superconducting cavities were also very stable with the acceleration gradient of 7 MV/m. The refrigerator for superconducting cavities had a few troubles, but these were not serious and the downtime was less than several hours.

The beam emittance after the injector cavities was measured for low bunch charge and for high bunch charge. For low bunch charge operation with 10 fC, the transverse normalized emittance was 0.17 mm mrad. This was slightly larger than the expected value of 0.1 mm mrad by particle tracking simulation without space charge effect. Figure 4 shows the beam profiles for low bunch charge operation. For high bunch charge operation with 7.7 pC, the emittance was less than 0.8 mm mrad, which depends on the condition of the beam transportation; this was larger than the expected value of 0.3 mm mrad by particle tracking simulation with space charge effect. For high bunch charge operation, we did not allow enough time for fine beam tuning. In the next beam operation, we plan to perform fine beam tuning around the injector superconducting cavities to reduce the emittance growth.

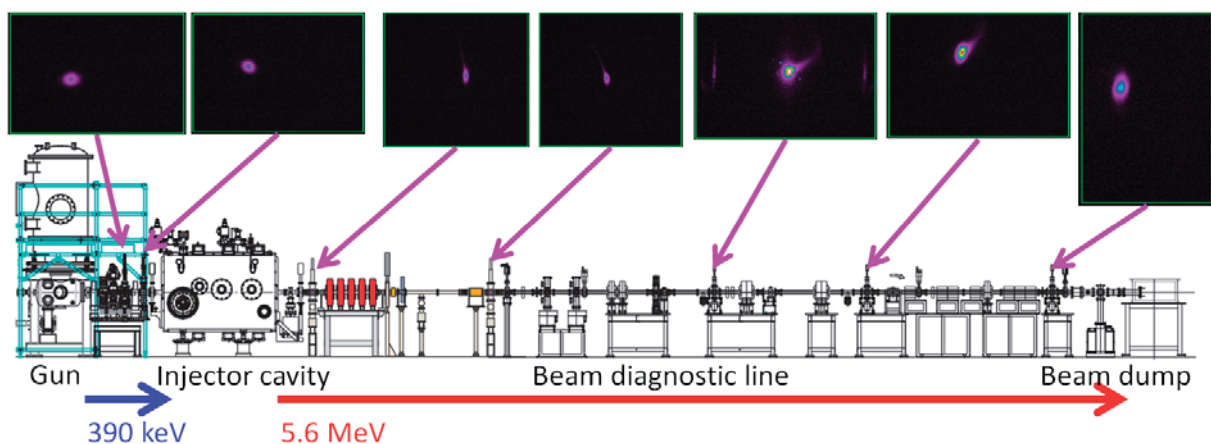


Figure 4: Transverse beam profiles in beam commissioning of cERL injector. The profiles were measured at screen monitors. Average beam current and bunch charge were 150 pA and 20 fC, respectively.

2-2-2. Commissioning of Recirculation Loop

The arc section of the recirculation loop consists of four 45-degree bending magnets and two quadrupole triplets, in which the beam optics are designed to make it isochronous and achromatic. The layout of the recirculation loop is shown in Fig. 5. A straight section between the two arc sections includes a pathlength control chicane and an interaction point of laser inverse Compton scattering. The injection beam is transported to the main linac through the injection chicane and merges with the recirculation beam. The recirculation beam is decelerated down to the injection energy, and then led to the main dump through the dump chicane.

The beam commissioning of the recirculating loop was performed for almost two months from Dec. 2013 to Mar. 2014 (including a one-month shutdown). The applied voltage of the DC electron gun is 390 kV, the same as was used during injector commissioning. During beam tuning, the average beam current is kept at less than 1 nA with a bunch charge of 10–100 fC and a pulse duration of 1 μ s. The acceleration field of the main cavity is limited to 8.5 MV per cavity to avoid increasing the radiation dose outside the accelerator room due

to field emission. Concerning the kinetic momentum of the electron beams, the ratio of the injection to the recirculation beam should be less than seven because the physical aperture is limited by the vacuum chamber of the chicanes. Accordingly, the injection and recirculation energy are set to 2.9 MeV and 20 MeV, respectively.

In the first week, we succeeded in accelerating the electron beam up to 20 MeV with the two cavities, which was confirmed at the 45-degree bending magnet. Stability factors of the low-level RF during beam operation were less than 0.02% in amplitude and 0.02 degree in phase, which satisfy the requirements of cEERL. However, the decelerated beam failed to reach the main dump because the leakage magnetic field of BMAG05 in Fig. 6 kicked the injection beam during the orbit tuning of the recirculation beam. In addition, it was found that the magnet of the cold cathode gauges (CCGs) kicked and distorted the low-energy injection/dump beam (Fig. 7). To remove such an unwanted magnetic field, a magnetic shield was added in the injection/merger chicane during the beam shutdown in Jan. 2014 and some CCGs were removed without serious effect on vacuum monitoring.

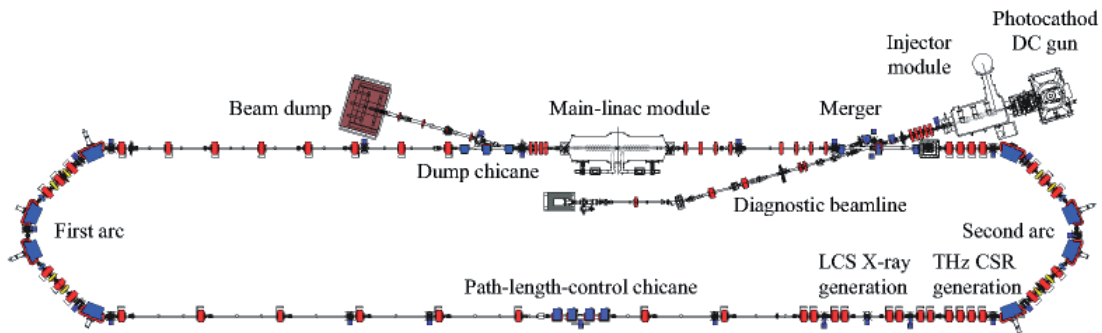


Figure 5: Illustration of the cEERL.

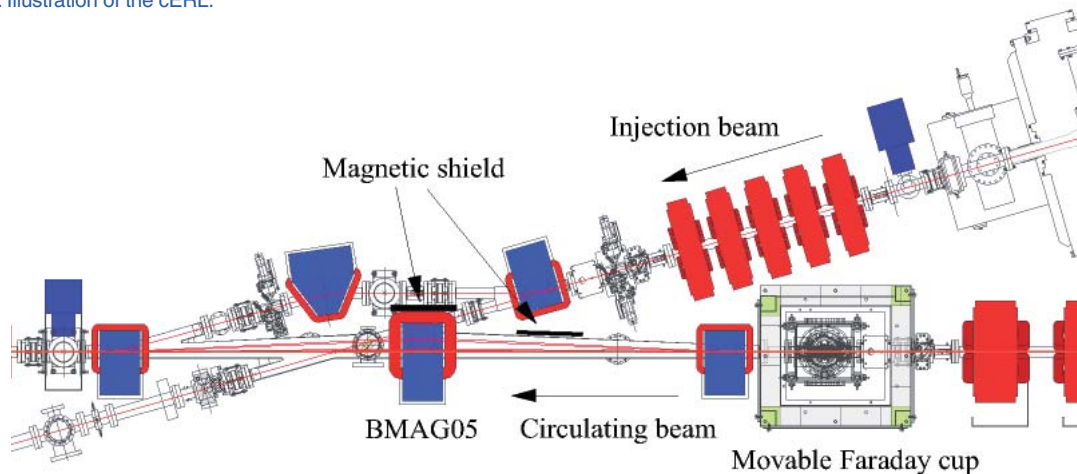


Figure 6: Effects of magnetic field of BMAG05 on the 2.9-MeV injection beam. Iron plates are effective as a magnetic shield.

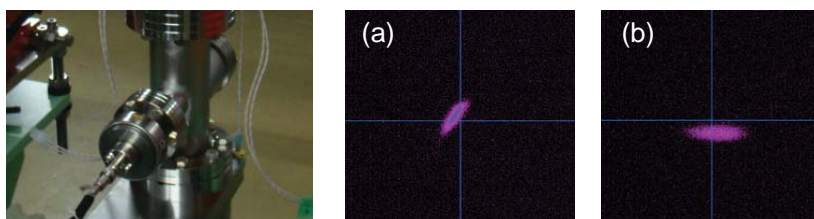


Figure 7: Left: Magnet of CCG (20 cm from chamber) Right: Beam profile (a) before and (b) after removing CCG and optics matching.

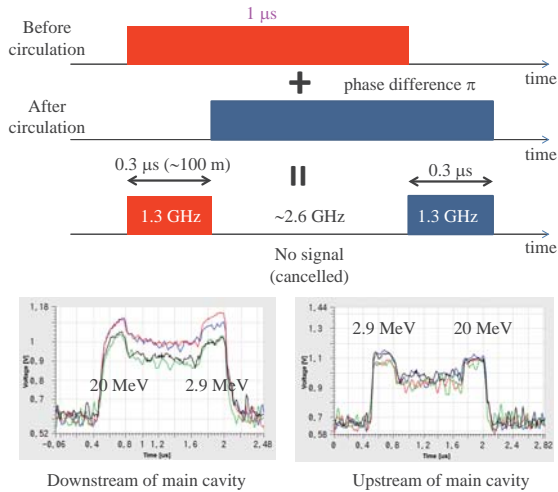


Figure 8: BPM signal of two accelerated and decelerated beams during burst operation. The signal is not completely cancelled even during the time period when both beams exist because the velocity of 2.9-MeV electrons is slightly different from the velocity of light.

In the region from the merger chicane to the dump chicane, it is impossible to monitor the circulation beam with an invasive beam diagnostics tool such as a screen monitor. Therefore, to distinguish the recirculation beam from the injection beam, a strip-line BPM as a non-invasive monitor was utilized in a burst mode operation. In principle, BPM with a 1.3-GHz bandpass filter is insensitive to the 2.6-GHz beam signal, in which the recirculating beam is out of phase with the injection beam by π . However, the head (tail) of the rectangular burst pulse transports the main linac without accompanying the recirculating (injection) beam as shown in Fig. 8. The temporal duration of the head (tail) is almost 300 ns with the recirculation loop of 92 m. This duration is long enough to distinguish the two beam position signals. Orbit tuning of the two beams is enabled by the simultaneous measurement with BPM and the decelerated beam was successfully observed at the main dump in a week. Figure 9 shows the beam profiles on the screen monitors and signals of Faraday cups in Feb. 2014. There is no significant beam loss in the recirculation loop according to the beam current measured by three Faraday cups, which are located at the DC electron gun, the exit of the second arc (Fig. 6) and the main dump. The en-

ergy of the dump beam is close to that of the injection beam, which is assumed from the bending radius of the BMAD01 (in Fig. 11).

To increase the efficiency of the energy recovery, the recirculation beam needs to match the deceleration RF phase of the main cavity. Therefore, fine tuning of the pathlength of the recirculation loop (recirculation time) is demonstrated with (a) a path-length chicane and (b) steering magnets of the second arc in Fig. 10. The pathlength was optimized to minimize the dump energy because the average beam current at the beam tuning is too low to observe the beam loading at the main cavity. The results are shown in Fig. 11. The bending angle of BMAD01 has a maximum value, in which the dump energy is assumed to be close to a minimum value.

After completing the beam tuning, 6.5 μA CW operation was demonstrated to observe the beam loading of the main cavity. The results are shown in Fig. 12. “Energy recovery test” means the normal operation of ERL. “Beam loading test” is another test, in which the electron beam is accelerated with the upstream cavity and then decelerated with the downstream cavity to lead into the main dump. There is no energy recovery in the latter test, which is performed as a reference. The difference between the input and reflection RF power, $\Delta(\text{Pin-Pref})$, in both tests is compared in Fig. 12. In the beam loading test, $\Delta(\text{Pin-Pref})$ of the upstream cavity has a positive value when the beam current exists. This means that input RF power is necessary in order to accelerate the electron beam without energy recovery. The downstream cavity receives the power from the decelerated electron beam, and vice versa. In contrast, $\Delta(\text{Pin-Pref})$ is constant regardless of the electron current in the energy recovery test. This proves that the power of the decelerated beam is recovered at the main cavity.

There are still problems concerning optics tuning and matching. We found that the beam response of some quadrupole magnets did not match the magnetic field measurements. In addition, unknown xy coupling appeared. Therefore, the single-kick response and the dispersion function of the two arc sections are slightly different from the design optics. These problems are now being investigated.

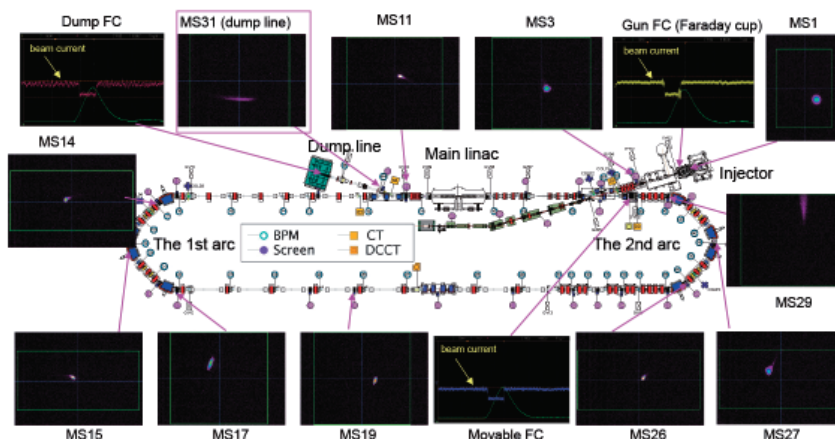


Figure 9: Beam profiles on the screen monitor and signals of Faraday cups (Feb. 2014).

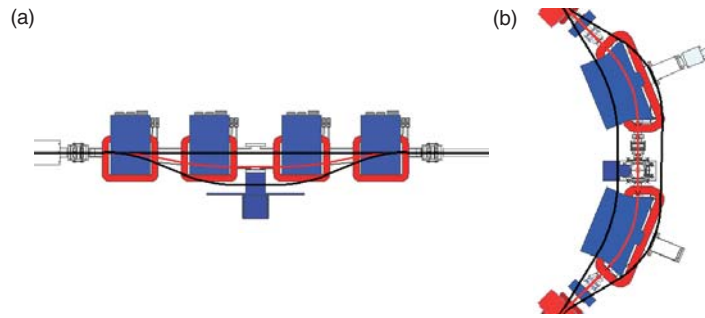


Figure 10: Magnetic pathlength control. (a) Chicane in the recirculation loop, (b) Combination of the steering magnet at the top of the second arc.

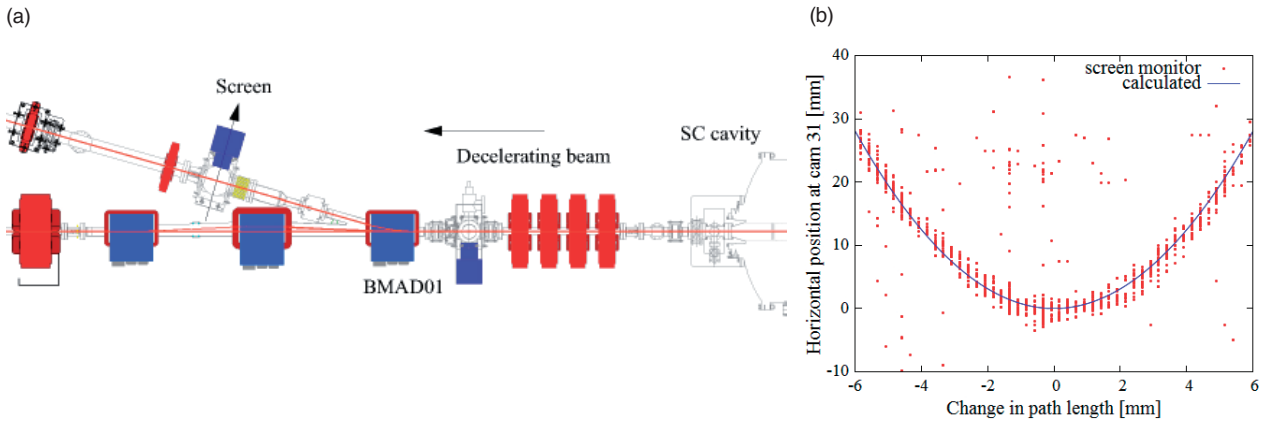


Figure 11: (a) Schematic of lattice layout at the dump chicane. (b) Plot of horizontal beam position at the screen (cam31) vs. pathlength of recirculation loop.

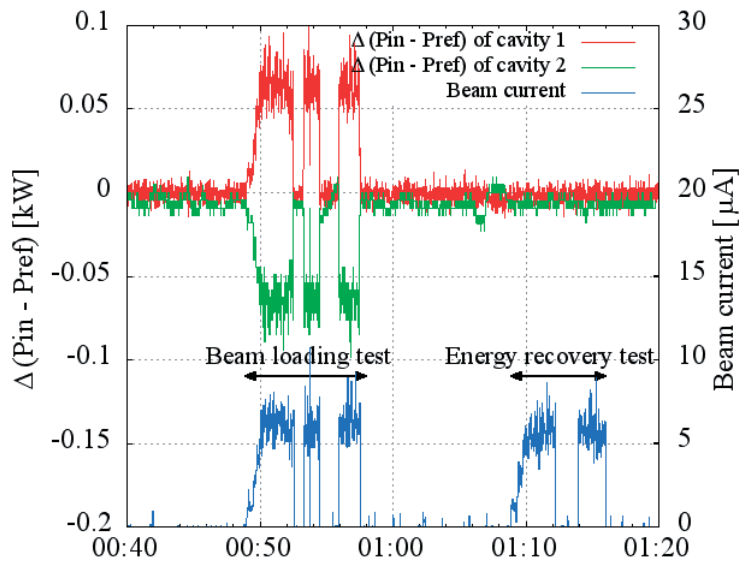


Figure 12: Plot of difference between the input and reflection RF power of the main linac, $\Delta(P_{in}-P_{ref})$ in the energy recovery test and the beam loading test. Cavity 1 and 2 mean the upstream and downstream cavity, respectively.